

Interactions between Se, Cs and Si upon Se adsorption on Cs/Si(111)-7×7 surfaces

This article has been downloaded from IOPscience. Please scroll down to see the full text article.

2002 J. Phys.: Condens. Matter 14 5255

(<http://iopscience.iop.org/0953-8984/14/21/301>)

View [the table of contents for this issue](#), or go to the [journal homepage](#) for more

Download details:

IP Address: 171.66.16.104

The article was downloaded on 18/05/2010 at 06:43

Please note that [terms and conditions apply](#).

Interactions between Se, Cs and Si upon Se adsorption on Cs/Si(111)- 7×7 surfaces

A C Papageorgopoulos and M Kamaratos

Department of Physics, University of Ioannina, PO Box 1186, GR-451 10 Ioannina, Greece

E-mail: me00426@cc.uoi.gr (A C Papageorgopoulos)

Received 3 January 2002, in final form 17 April 2002

Published 16 May 2002

Online at stacks.iop.org/JPhysCM/14/5255

Abstract

This report involves the room and elevated temperature ultrahigh-vacuum study of Se adsorbed on caesiated Si(111)- 7×7 surfaces using Auger electron spectroscopy, low-energy electron diffraction, work-function measurements and thermal desorption spectroscopy. Adsorption of Se on Cs/Si(111)- 7×7 surfaces initially occurs on the uncaesiated portions of the Si substrate and subsequently on the Cs adatoms. Heating the Se/Cs/Si(111)- 7×7 surface causes Se to diffuse below the Cs adlayer to form strong dipoles with the alkali metal adatoms. The presence of Se increases the energy of binding of Cs to the substrate, and $\text{Cs}_x\text{Se}_y\text{Si}_z$ compound formation was observed with a binding energy of 2.8 eV/atom. The Cs–Se bonds most probably break at 1050 K, and two binding states of Cs and Se were observed after heating to temperatures >1050 K. Their calculated binding energies are 3.0 and 3.2 eV/atom. The coadsorption of Cs and Se induces a high degree of surface disorder, while desorption most probably causes surface etching. Finally, the presence of Cs on the Si(111)- 7×7 surface greatly suppresses the formation of SiSe_2 , detected when Se is adsorbed on clean Si(111)- 7×7 surfaces.

1. Introduction

In contrast to the case for other elements in group VI, such as oxygen and sulphur, adsorption studies of Se on Si surfaces are very scarce [1–7]. Semiconductor compounds of Se, however, have been receiving increased attention lately, due to their unique optical, structural and electrical properties [8, 9]. Deposition studies of compounds such as ZnSe, InSe and GaSe have been recently performed on surfaces of Si [3, 7, 8], yet there have been no investigations regarding the coadsorption of their constituent elements which may provide additional valuable information regarding their applicability.

Two-dimensional systems of coadsorbed electropositive alkali metals and electronegative nonmetallic elements of group VI on semiconductor and metallic surfaces, moreover, have

important technological applications in thermionic energy conversion, microelectronics and the construction of photocathodes [10–12]. Specifically, coadsorption of alkali metal atoms and oxygen is known to reduce the work function (WF) of metal and semiconductor surfaces [13, 14], of primary importance in applications. Deposited alkali metals are known to promote oxidation on metallic and semiconductor surfaces as well as increasing the amount of oxygen which can be adsorbed onto the surface [15, 16]. Despite the scientific and technological interest, investigations on the coadsorption of alkali metals and chalcogen group VI elements are limited, to our knowledge, to alkali metals adsorbed with S onto Ni(100) and Si(100) surfaces [17–19].

The properties of the Si(111)- 7×7 surface, and its heat-induced $7 \times 7 \rightarrow 1 \times 1$ phase transition, have been thoroughly studied in the past [20]. This is one of the most complex surfaces of silicon, and it exhibits a rich variety of reconstructions with different adsorbates [21]. It is not surprising, therefore (given also its applicability in industry), that the Si(111)- 7×7 surface has been the subject of many adsorption and coadsorption studies [21, 22]. To our knowledge, however, there are no reports on the effects of simultaneous coadsorption of Se with any other element on this surface.

This investigation, in particular, studies the adsorption of Se on caesiated Si(111)- 7×7 surfaces at room and elevated temperatures. Data were acquired using the surface analysis techniques of Auger electron spectroscopy (AES), low-energy electron diffraction (LEED), thermal desorption spectroscopy (TDS) and WF measurements. To better understand the combined interactions of Se and Cs on Si(111)- 7×7 surfaces, it is necessary to understand the behaviour of Se on the clean Si(111)- 7×7 surface, and also of Cs on Si(111)- 7×7 , which we briefly describe below.

Se adsorbed on clean Si(111)- 7×7 . The earliest study of Se on the Si(111)- 7×7 surface was done by Dev *et al* [1]. Selenium was deposited onto a chemically cleaned Si(111) surface using a weakly acidic methanol solution. After analysis using x-ray standing-wave (XSW) interference spectrometry, the authors subsequently proposed that Se atoms occupy the bridge sites between adjacent Si atoms on the Si(111) surface. Their study revealed that Se passivates the latter surface, which in their case remained stable for 12 h under atmospheric conditions.

In a very recent study by Shuang Meng *et al* [7], utilizing LEED, x-ray photoelectron spectroscopy (XPS) and x-ray photoelectron diffraction (XPD), Se was deposited on the Si(111)- 7×7 surface at RT, with subsequent annealing at $\sim 400^\circ\text{C}$, as well as directly at 450°C . It was observed that Se adsorption on Si(111)- 7×7 leads to a disordered surface Se layer with little or no interdiffusion. The authors of this work have also investigated the room and elevated temperature adsorption of Se on Si(111)- 7×7 surfaces with the same techniques as are used in this coadsorption study [6]. Se was deposited, *in situ*, by thermal dissociation of WSe_2 . In the subsequent report it was proposed that Se initially adsorbs onto the top surface layer up to a coverage of 0.50 ML (corresponding to about 25 Se atoms per substrate unit cell). For increasing coverages, Se diffuses below the surface, and upon subsequent heating to 1025–1050 K, Se desorbs in the form of SiSe_2 . When the Se/Si(111)- 7×7 surface is heated to 1050 K, the 7×7 surface becomes 1×1 , remaining so even at RT, while the 0.50 ML Se overlayer is disordered.

Cs adsorbed on clean Si(111)- 7×7 . For Cs deposited on Si(111)- 7×7 surfaces at a coverage up to 0.15 ML, Magnusson *et al* [23] have suggested that binding occurs primarily to the adatom sites and secondly to the rest-atom dangling bonds, while the work of Etelaniemi *et al* [24] concludes that, at saturation coverage, both the topmost (adatom) and threefold (rest-atom) sites

are filled. The completion of a physical (saturation) layer would then amount to 18 atoms per unit cell. Etelaniemi *et al.*, however, believe that the order of site preference is reversed, with the threefold sites being the first preference. This conclusion is supported by recent optical second-harmonic-generation measurements [25], as well as theoretical calculations [26]. Energy calculations for various adsorbates on the Si(111)-7 × 7 surface have, furthermore, led Cho and Kaxiras [27] to conclude, at least for low coverages, that adsorbate atoms are not likely to attach to dangling bond sites (either rest-atom or adatom sites). Theoretical calculations have, furthermore, shown that the bonding of Cs to Si(111) surfaces, at low coverages, has a strong ionic character [28,29], which is in agreement with most of the experimental findings [29,30]. For higher coverage, approaching saturation, it has been established that the Cs/Si(111) surface becomes metallic [23–25, 28–30, 32]. This metallic state for Cs on Si(111)-7 × 7 is usually understood in terms of the competition between Cs–Cs and Cs–Si interactions, and may not be fully developed with respect to pure metallic Cs [23, 30–32].

The authors of the current investigation are in partial agreement with the Magnusson structural picture. In a recent work, comparing Cs coverages of Si(111)-7 × 7 with those of surfaces where saturation coverage is known, it was observed that Cs saturates the Si(111)-7 × 7 surface at RT at 0.47 ML [33]. Utilizing comparisons between AES measurements, LEED and WF change observations it was, furthermore, suggested that Cs adatoms prefer the outermost dangling bonds until they saturate them at about 0.23 ML. Thereafter, however, site preference is random and continued adsorption of Cs on the Si(111)-7 × 7 surface leads to a disordering of the latter. As for the degree of metallicity of a physical layer of Cs on Si(111)-7 × 7 surfaces, the calculation of the binding energy of the metallic peak of the TDS spectrum of Cs, and the WF of the saturated layer both revealed a near-metallic state for Cs, in agreement with the previous findings [23,30–32]. The analysis of the interactions of Se, Cs and Si are based on the above results, which are presented schematically in figure 1. Figure 1(a), in particular, depicts the probable arrangement of Cs adatoms on the Si(111)-7 × 7 surface when $\Theta_{\text{Cs}} \cong 0.23$ ML (half the saturation coverage), according to the model proposed by the authors [33]. Figure 1(b), on the other hand, shows Cs adsorbed on an ordered Si(111)-7 × 7 substrate for convenience of illustration, even though LEED observations indicated a lack of surface periodicity. In reality, results (represented by figure 1(b)) suggest that Cs accumulates, as shown, in the central domains of the Si(111)-7 × 7 unit cells interacting strongly with the substrate, and generating the observed disorder without losing their positions. The results described below utilize the model indicated in figure 1. It should be noted that the Cs atoms (depicted with a bold circumference) are of smaller radius in the top portion of figure 1 than in the bottom portion. As marked in the figure, the Cs adatoms at the top correspond to Cs with an ionic character, and hence radius, while those of the bottom correspond to a near-metallic character (with greater radius).

2. Experimental methods

The experiments were performed in an ultrahigh-vacuum (UHV) chamber, with a base pressure below 10^{-10} Torr. The chamber was equipped with AES, LEED, TDS and WF measurement apparatus. The diode method was used for measuring changes in the WF, with an error margin of ± 0.01 eV. Cesium was evaporated from a commercial dispenser source (SAES getters). The quadrupole mass spectrometer (QMS), utilized for TDS, was calibrated with a heating rate of $\beta = 17$ K s⁻¹. Seebauer's formula was used to calculate the binding energies corresponding to the respective desorption temperatures, with an error $< \pm 0.1$ eV/atom [34]. Elemental Se was evaporated by thermal dissociation of WSe₂ enclosed in envelopes of thin Ta plates which were heated by passing the required electrical current. During dissociation, the W remained in the

Si(111) 7x7

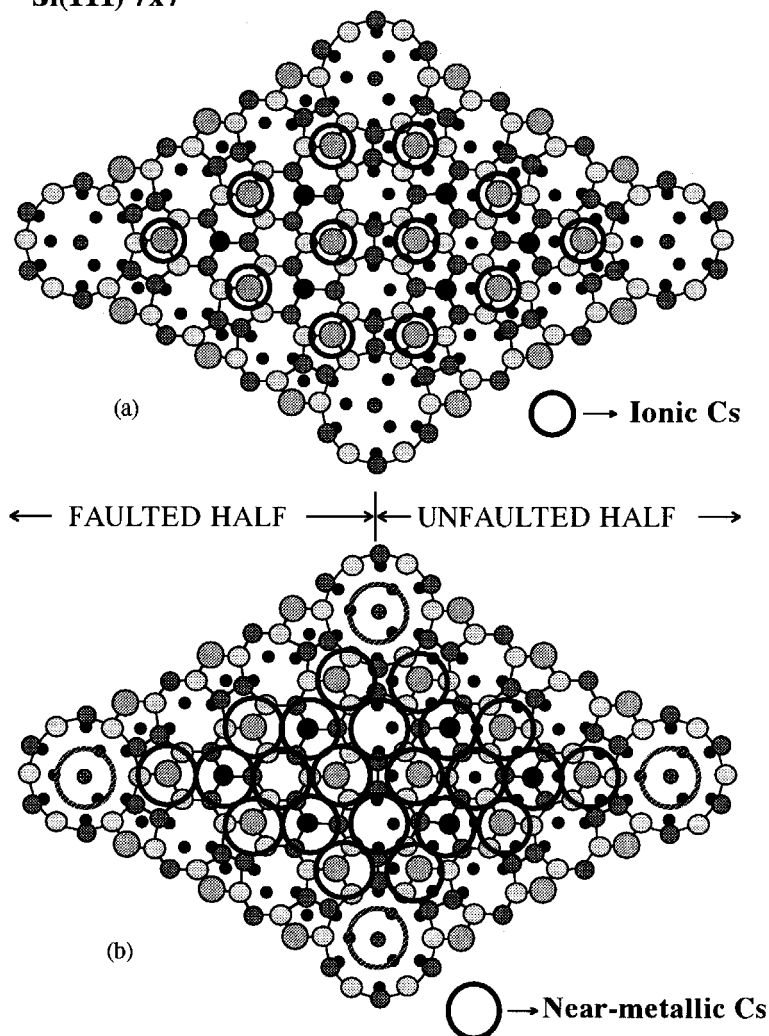


Figure 1. (a) is a schematic diagram of 0.23 ML of Cs deposited at RT on the Si(111)-7 × 7 surface according to the model proposed by the authors. The ionic radius of Cs is depicted. (b) is a schematic diagram of ~0.47 ML (saturation layer) of Cs deposited at RT on the Si(111)-7 × 7 surface, according to the same model. The Cs size here corresponds to the metallic radius of Cs. (The surface disorder observed in case (b) is not taken into account.) Cesium adatoms are shown as bold hollow circles. The broken circles depict a speculated corner hole site contribution by Cs.

Ta envelope, while Se was evaporated through holes made at the edge of the Ta enclosure. The atomic Se was an estimated 30% of the total yield. The estimation was done by first plotting the QMS signal intensity versus time, for both atomic and molecular Se, with a constant current running through the Ta envelope, and thereafter comparing the areas under these graphs.

The respective dosages of Cs and Se were calibrated by analysing LEED, WF and AES data for the adsorbates, separately deposited at RT on a Si(100)-2 × 1 substrate. The surface atomic density of a saturation layer (1 ML) of Cs [30, 31] was considered equal to that of the outermost layer of the Si(100)-2 × 1 surface, $N_{\text{Si}(100)} = 6.8 \times 10^{14} \text{ atoms cm}^{-2}$, while the

surface atomic density of Si(111)-7 × 7 is $N_{\text{Si}(111)} = 7.8 \times 10^{14}$ atoms cm^{-2} . The amount of Cs per dose was then estimated (in terms of atomic surface density) using the Si(100)-2 × 1 surface. The coverage for the maximum amount of Cs accepted by the Si(111)-7 × 7 surface was, then, estimated at 0.47 ML. The estimation of the dosage for Se was done according to previous studies of Se adsorbed on Si(100)-2 × 1 and Si(111)-7 × 7 surfaces [5,6]. The Si(111)-7 × 7 and Si(100)-2 × 1 surfaces were cleaned by annealing at 1000 K, and surface purity was verified by AES. The temperatures of the samples were measured by a Cr–Al thermocouple calibrated with an infrared pyrometer in the range 900–1300 K.

3. Results and discussion

LEED/Auger. The clean Si(111)-7 × 7 surface produced the well known 7 × 7 reciprocal-lattice pattern. As mentioned, saturation coverage (0.47 ML) of Cs induces a high degree of disorder on the Si(111)-7 × 7 surface. At a primary electron energy of 38 eV, spots disappeared, including the primaries. The primary spots reappeared when the electron energy was increased to 47 eV, although the background remained high, with streaks along the directions connecting the first-order spots, indicating that the disorder is most probably restricted to the top two surface layers. Twenty doses of Se were, subsequently, added at RT, and were calibrated to correspond to an equivalent coverage of 1.0 ML. The only observable change was a noticeable increase in the background, and the disappearance of the streaks. At the low-penetration-depth beam energy of 40 eV, faint first-order spots were observable, most probably indicating that disorder was restricted at most to the first two atomic layers. Gradual heating of the sample to 1300 K followed, and observations of the LEED pattern were made every 100 K. There was no observable change in the pattern up to 900 K, whereupon first-order spots began to appear more clearly, and the background intensity began to decrease. By 1100 K the first-order spots were very clear, and the background intensity was considerably lower than before heating. Between 1100 and 1300 K the seventh-order spots began to appear, with the 7 × 7 pattern becoming clear by the latter temperature.

Figure 2 (left) shows the Auger peak-to-peak heights (Ap–pH) of Si (91 eV) and Cs (563 eV) (top and bottom portion respectively), as a function of the doses of Se, which were deposited at RT onto a 0.47 ML Cs-covered Si(111)-7 × 7 surface. Dosage was calibrated at 0.1 ML per dose (as with LEED), with a total of 16 doses (1.6 ML) deposited. The Cs (45 eV) and Se (47 eV) peaks could not be reliably resolved due to their close proximity. We, therefore, measured the Ap–pH changes relative to increasing coverage of the Cs (563 eV) peak. For the first five doses the latter peak intensity remained constant, and thereafter it exhibited a gradual decrease until the 14th dose was given, whereupon it stabilized. Initially, the Si (91 eV) peak decreases drastically up to the third dose. Thereafter, the peak intensity decrease occurred in a more gradual manner until the Si (91 eV) peak almost disappeared. By correlating the behaviours of the measured Si and Cs Ap–pH changes (i.e. the former's change in rate of decrease and the latter's constancy), we conclude that the first 0.50 ML of deposited Se (left side of figure 2) most probably initially adsorbs on the exposed portions of the Si substrate (first three doses). The area of initial adsorption for Se is most probably that which surrounds the central domain of the 7 × 7 unit-cell area, where there would be no masking of the Cs adatoms. After the third dose, a second Se adlayer may begin to form on top of the first. Selenium adsorption onto the central domain, where it begins to cover the Cs adatoms as well as the Si substrate, most probably occurs when $\Theta_{\text{Se}} > 0.50$ ML, i.e. as the Cs (563 eV) peak intensities begin to decrease (figure 2, lower left).

The heating of the sample from RT (~300 K) to 1300 K is depicted on the right, with the plot of the Ap–pH versus temperature (in kelvins) of the Si (91 eV) peak in the top portion

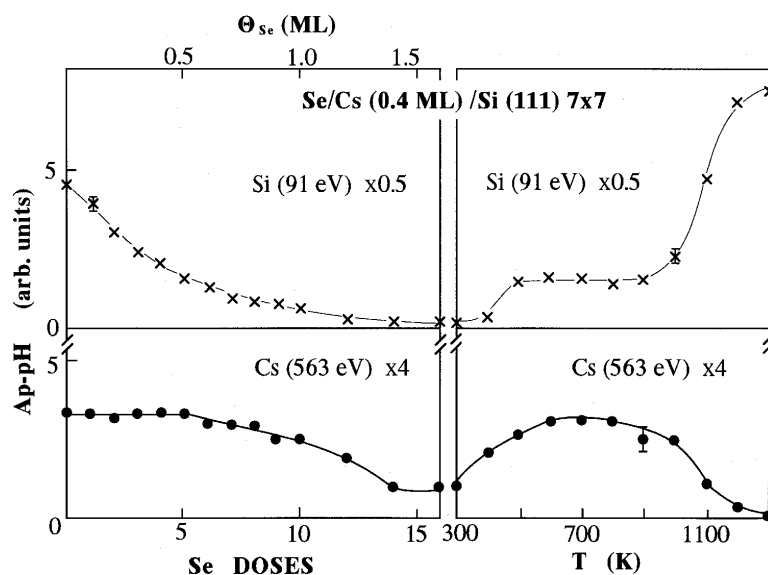


Figure 2. This figure shows (left) the Auger peak-to-peak heights (Ap-pH) of Si (91 eV) and Cs (563 eV) (top and bottom portions respectively), as a function of the doses of Se, which were deposited at RT onto a 0.47 ML Cs-covered Si(111)-7 \times 7 surface. On the right we show the heating of the sample from RT (300 K) to 1300 K with the plot of the Ap-pH versus temperature (in kelvins) of the Si (91 eV) peak in the top portion and the Cs 563 eV peak at the bottom. Auger spectra were taken every 100 K.

and the Cs (563 eV) peak at the bottom. Auger spectra were taken every 100 K. Between the temperatures of 400 and 500 K the Si (91 eV) peak intensity undergoes a relatively sharp increase and stabilizes up to about 900 K, whereupon it increases again until the final intensity value is reached at 1300 K, marking the desorption of all adsorbates. The Cs (563 eV) peak, on the other hand, increases until 600 K, remains stable until 800 K and subsequently decreases until it disappears at 1200 K. The above variations of the measured Ap-pHs of the heat-treated Se/Cs/Si(111)-7 \times 7 surface indicate a structural rearrangement at 400–500 K, which increases the peak intensities of Si as well as those of Cs. By 600 K the Cs peak intensities have reached the same values as those before Se was deposited at RT, which suggests that Cs has moved to the topmost positions, with Se adatoms diffusing underneath as well as occupying portions of the surface devoid of Cs adatoms. The likelihood of the aforementioned behaviour is supported by the observed variations in the Cs (563 eV) and Si (91 eV) Ap-pH intensities in the 500–900 K range. This equals the intensities of the corresponding Ap-pHs at the fifth Se dose at RT (0.50 ML). The proposed behaviour is also supported by the results of the WF measurements reported below.

WF changes. Figure 3 (left) is a graph of the WF changes of Se on clean and Cs-covered Si(111)-7 \times 7 surfaces, as a function of Se dose at RT. The coverage of Se was calibrated at approximately 0.08 ML/dose, from the WF changes of Se on clean Si(111)-7 \times 7 [6]. It is primarily evident that in all the curves depicting the WF changes of Se on Cs/Si(111)-7 \times 7 surfaces, Se increases the WF to a near-constant value. The initial deviations in the slope of the WF curve of Se on clean Si(111)-7 \times 7 have been attributed to site preference, and the change in slope at the tenth dose was interpreted as an indication of Se diffusing into the substrate bulk [6]. When $0.02 \text{ ML} \leq \Theta_{Cs} \leq 0.15 \text{ ML}$, the WF curves exhibit similar

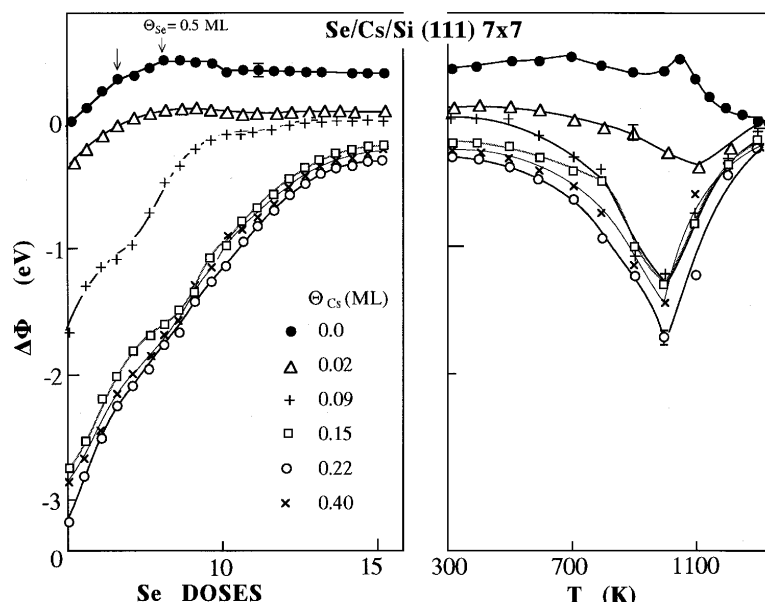


Figure 3. On the left we show a graph of the RT WF changes of Se on clean and Cs-covered Si(111)-7 × 7 surfaces, as a function of Se dose. On the right are the WF changes as a function of temperature. The Se/Si(111) and Se/Cs/Si(111) surfaces which gave the room temperature WF changes were, specifically, heated in 100 K intervals, from 300 to 1300 K, and the WF changes noted at RT.

slope changes around the third and sixth Se doses, most probably due to the Se preferring to adsorb on or near the same sites as on the clean surface. This behaviour is expected since, according to the previously proposed model (figure 1(a)), Cs prefers to adsorb on the adatom dangling bonds up to a coverage of $\Theta_{\text{Cs}} \cong 0.23$ ML [33]. At Cs coverages above 0.15 ML, surface disorder increases dramatically (symmetry is lost at $\Theta_{\text{Cs}} > 0.23$ ML) and the question of Se site preference ceases to be an issue. The WF changes of the left side of figure 3, furthermore, do not provide any evidence of formation of RT chemical compounds of the adsorbates.

When Se coverage reaches 0.50 ML, the WF of the Se/Si(111)-7 × 7 surface remains constant, and subsequently decreases with increasing dosage, which was attributed to the onset of Se diffusion below the surface [6]. The presence of Cs delays the WF stabilization to even larger Se coverages. When $\Theta_{\text{Cs}} \cong 0.47$ ML, the WF curve stabilizes at the 15th or 16th dose (figure 3, left), in agreement with the AES data for corresponding adsorbate coverages (figure 2, left). Thereafter Se may diffuse below the Cs adlayer, and possibly below the top disordered layers of the Si(111) substrate. It is most likely, as indicated by the above observed delay in the stabilization of the WF curves at higher adsorbate coverages, that Cs saturation coverage increases the amount of Se remaining on the surface from 0.50 to 1.50 ML (~200%), i.e. Cs inhibits diffusion of Se into the Si(111) bulk.

The WF changes as a function of temperature are shown on the right side of figure 3. The Se/Si(111) and Se/Cs/Si(111) surfaces which gave the room temperature WF changes were heated in 100 K intervals, from 300 to 1300 K, and the WF changes noted at RT. The variations of the heated Se/Si(111) surface are depicted at the top of the figure, and below this are the plots corresponding to the heating of the Se/Cs/Si(111) surfaces depicted on the left side of figure 3. There is a marked difference between the WF changes of Se on the clean surface

and those of Se on the caesiated surfaces. The point of interest is the WF minimum at about 1000 K when $\Theta_{\text{Cs}} \geq 0.09$ ML, in contrast to the maximum in the WF of the heat-treated Se/Si(111) surface. The minimum of the caesiated surface signifies an increase in the dipole moment, whose vector points in the positive direction (upwards), i.e., from surface to vacuum. The WF versus temperature plot substantiates the surface rearrangement observed in the AES data of figure 2, right, which suggests that Cs adatoms have moved to the topmost positions on the surface, whereas removal of adsorbates commences at temperatures corresponding to the observed minimum of figure 3, right. The lowest WF measured was $\Delta\Phi = -1.7$ eV, when 1.5 ML of Se was deposited onto 0.26 ML of caesiated Si(111)- 7×7 , approximately at the Cs/Si(111)- 7×7 WF minimum. The surface structure for Cs/Si(111)- 7×7 at the minimum is depicted in figure 1(a).

TDS. TDS was performed on Se/Si(111)- 7×7 and Se/Cs/Si(111)- 7×7 surfaces at various coverages of Se and Cs, for the detection of Se (79 amu), Cs (133 amu), SiSe (107 amu), SiSe₂ (186 amu), CsSe (212 amu), CsSeSi (240 amu) and CsSeSi₂ (268 amu). The upper atomic mass limit of 300 amu, unfortunately, prevented the detection of larger molecules. The aforementioned spectra are depicted in figures 4–8 (the spectra of CsSe are not shown in this work). All thermal desorption spectra (TDS) are plots of the QMS signal as a function of temperature in kelvins. During desorption, the temperature increased from 300 to over 1300 K at a constant rate of 17 K s⁻¹. The QMS signal strengths were constant for each set of spectra, but varied from figure to figure. No comparisons in signal strength are, therefore, made between figures. It should also be noted that peaks corresponding to the detection of different desorbed species removed from the substrate at the same temperatures are given the same (letter) designations.

Figure 4 shows the TDS of Cs (133 amu) at saturation coverage on Cs/Si(111)- 7×7 and Se/Cs/Si(111)- 7×7 surfaces, with varying coverages of Se. A coverage of 0.50 ML of Se causes a drastic alteration of the characteristic heat-induced desorption curve of Cs on clean Si(111)- 7×7 , by shifting the desorption of Cs to higher temperatures. This implies that the presence of Se strengthens the binding of Cs to the substrate. When $\Theta_{\text{Se}} \geq 1.0$ ML three distinct binding states emerge, represented by the peaks marked α at 1210 K, α_1 at about 1100 K for $1.0 \text{ ML} \leq \Theta_{\text{Se}} \leq 1.5 \text{ ML}$ and α_2 at 1050 K, the latter of which is found to dominate the spectrum at coverages of Se over 1.0 ML. The observed increase in the degree of Cs binding to the substrate is most probably due to the prominent Se–Cs interaction leading to possible compound formation. Spectrum 4 of figure 4 corresponds directly to the WF curve of the heat-treated Se(1.5 ML)/Cs(0.47 ML)/Si(111)- 7×7 surface (figure 3, right). The comparison of these two sets of data confirms that the majority of the Cs of peak α_2 is removed during the subsequent increase of the WF (after attaining its minimum value) of the heated Se(1.5 ML)/Cs(0.47 ML)/Si(111)- 7×7 surface. This supports the proposal that the decrease of the WF depicted in figure 3, right, is solely due to the suggested structural rearrangement where Se diffuses below the Cs adatoms.

Figure 5 shows the TDS of Se (79 amu), desorbed from Se/Cs/Si(111)- 7×7 surfaces with Cs maintained at saturation coverage (0.47 ML), and Se at coverages of 0.33, 1.0 and 3.0 ML. The lowest Se coverage results in a high-energy peak, designated α , at about 1210 K, which grows in intensity with increasing Se coverage. At the Se coverage of 1.0 ML, the beginnings of two more peaks are evident at lower energies. These also become more prominent at higher Se coverage, and are designated as peaks α_1 and α_2 , at 1110 and 1050 K respectively. When 3.0 ML of Se covers the Cs/Si(111)- 7×7 surface, two more peaks emerge at even lower energies, besides the ones already mentioned. These are designated α_3 at about 970 K and α_4 at 600 K.

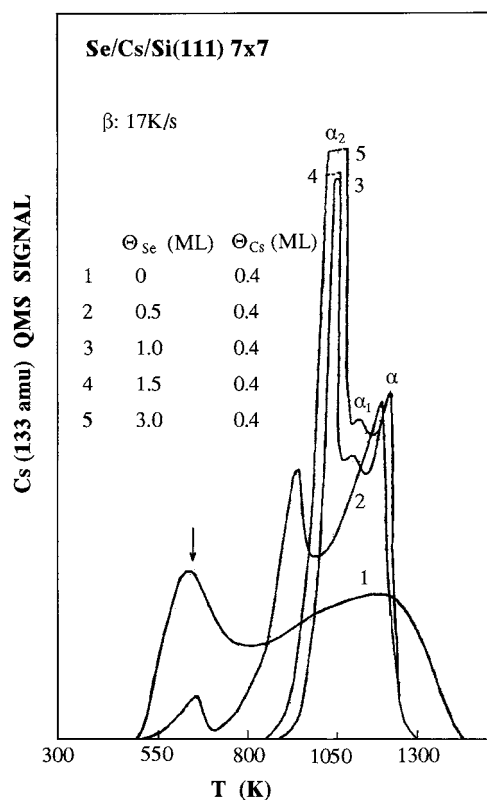


Figure 4. This figure shows the TDS of Cs (133 amu) at saturation coverage on Cs/Si(111)-7 × 7 and Se/Cs/Si(111)-7 × 7 surfaces, heated at a constant heating rate, between 300 and 1300 K with varying coverages of Se.

Figure 6 shows the TDS of SiSe (107 amu), desorbed from Se/Si(111)-7 × 7 and Se/Cs/Si(111)-7 × 7 surfaces. The coverage of Se is maintained at a constant 3.0 ML in all three cases, while the Cs coverage for the Se/Cs/Si(111)-7 × 7 surface was <0.02, 0.10 and 0.47 ML. There are four prominent desorption peaks for the latter surface, which correspond directly to the peaks α , α_1 , α_2 and α_3 of figure 5, and which become distinct at $\Theta_{\text{Cs}} \cong 0.47$ ML and $\Theta_{\text{Se}} \cong 3.0$ ML. The peak corresponding to α_4 , however, was not observed in the detection of SiSe. It should be noted that the coverage $\Theta_{\text{Cs}} < 0.02$ ML, for TDS curve 1 of this figure (corresponding to less than one dose of Cs), is due to trace amounts of Cs remaining on the substrate surface, even after heating to 1400 K, and undetectable by TDS. These traces, however, increase the intensity of the high-energy Se peak (which usually saturates at a ~ 0.50 ML Se coverage for the Se-covered Si(111)-7 × 7 surface). In other words, spectrum 1 of figure 6 shows that even small amounts of Cs drastically increase the amount of Se that is bound most strongly to the surface, represented by peak α . The implications of the above observation, which will be thoroughly discussed later in this report, may provide an explanation as to why there is no observed restoration after the Cs/Se/Si(111)-7 × 7 surfaces are heated to temperatures over 1050 K, even though most of the Cs has been removed from the surface (as indicated by figures 2 and 4). The comparison of figures 5, 6 (as well as figure 7, which will be discussed below) points to a common result: that the peaks α , α_1 and α_2 , which are present in all three TDS plots, are due to the detection of fragments of compounds containing

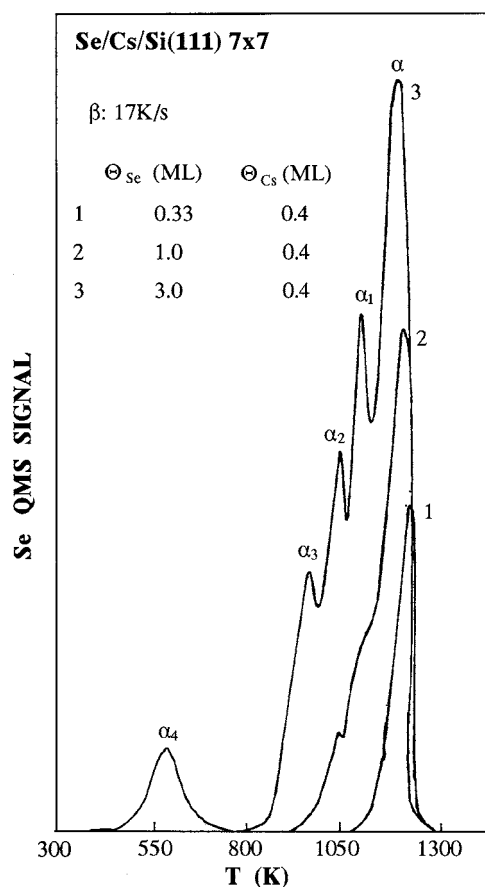


Figure 5. This figure shows the TDS of Se (79 amu), desorbed from Se/Cs/Si(111)-7 \times 7 surfaces, at a constant heating rate, between 300 and 1300 K. The cesium was maintained at saturation coverage (~ 0.47 ML), with the Se at coverages of 0.33, 1.0 and 3.0 ML.

the elements observed in each plot. The fragments were created from the splitting of the compounds within the QMS during the ionization process, which is part of its function. The following figures, where the presence of Cs–Se and Cs–Se–Si compounds is detected, confirm this result.

Figure 7 reveals the presence of two chemical formations. The series of spectra depicts the QMS signal strengths for CsSeSi (240 amu) and CsSeSi₂ (268 amu), as a function of temperature. Both formations were detected at 1050 K, which is the same as for previous observations of peak α . For Cs at saturation coverage, CsSeSi becomes dominant at Se coverages of over 1.0 ML, while at higher Se coverage CsSeSi₂ is the more dominant formation. The equivalent of the Se peak α_4 is also observed, appearing around 600 K for CsSeSi₂, while a similar low-temperature peak appears for CsSeSi. The spectra revealing the presence of CsSe are not shown here due to their similarity to the TDS plots of figure 7. There is a strong indication that heating the Se/Cs/Si(111)-7 \times 7 surface to 1050 K induces etching of the top surface layer, therefore removing portions of the substrate as well as the adsorbates. It is most probable that the detected CsSe is a portion of some larger molecules containing Cs, Se and Si, which had undergone fragmentation in the QMS.

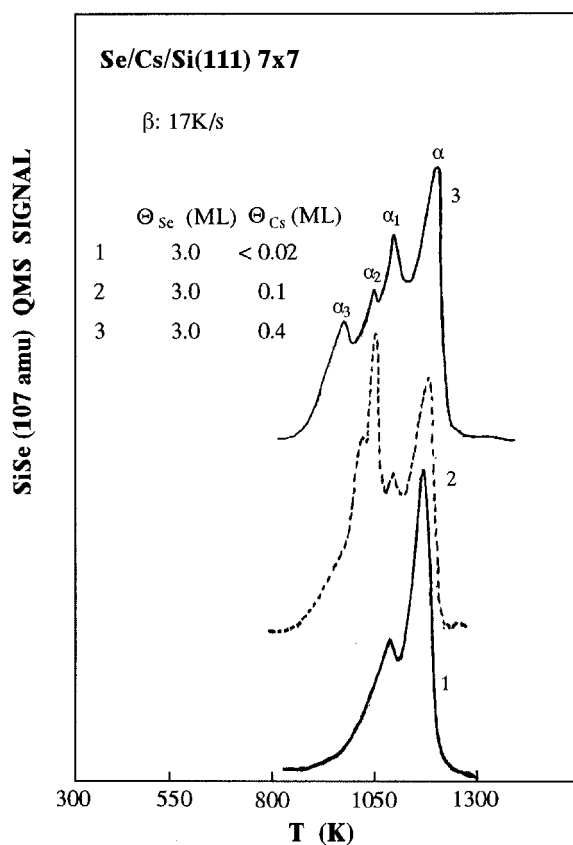


Figure 6. This figure shows the TDS of SiSe (107 amu), desorbed from Se/Si(111)-7 × 7 and Se/Cs/Si(111)-7 × 7 surfaces, at a constant heating rate, in a temperature range between 300 and 1300 K. The coverage of Se is maintained at a constant 3.0 ML in all three cases, while the Cs coverages for the Se/Cs/Si(111)-7 × 7 surface were <0.02, 0.1 and ~0.4 ML.

Figure 8 depicts the TDS of SiSe₂ (186 amu) desorbed from Se/Si(111)-7 × 7 and Se/Cs/Si(111)-7 × 7 surfaces. On the left of the figure, Se coverage remains at a constant 0.75 ML, which corresponds to nine doses on the WF plot of figure 3 (left). There are four consecutive spectra of increasing Cs coverage, from 0.02 to 0.25 ML, compared to the TDS of SiSe₂ desorbed from the Se/Si(111)-7 × 7 surface. On the right side of the figure are the TDS for 2.50 ML of Se deposited onto clean and Cs-saturated Si(111)-7 × 7 surfaces. The purpose of obtaining these two separate TDS sequences was to demonstrate the suppression of the formation of SiSe₂ by the presence of Cs at both low and high coverages of both adsorbates. In the low-coverage sequence (figure 8, left), we notice that the SiSe₂ peak is merely suppressed (i.e. the general shape of the peak does not alter). For high coverage of both adsorbates, however, there is in addition to the drastic decrease in intensity, also a doubling of the peak, which is also accompanied by a shift to higher temperatures (1075 and 1175 K).

In order to achieve a more comprehensive overall understanding of the results provided by TDS measurements, a more detailed discussion is in order, entailing a combined interpretation of the information provided in figures 1–8. As already mentioned, the three high-temperature peaks common to figures 4–7 and designated α , α_1 and α_2 , reveal the consecutive binding states of Se ($\Theta_{\text{Se}} > 1.0$ ML) and Cs, both deposited at RT, during heating, and are of particular

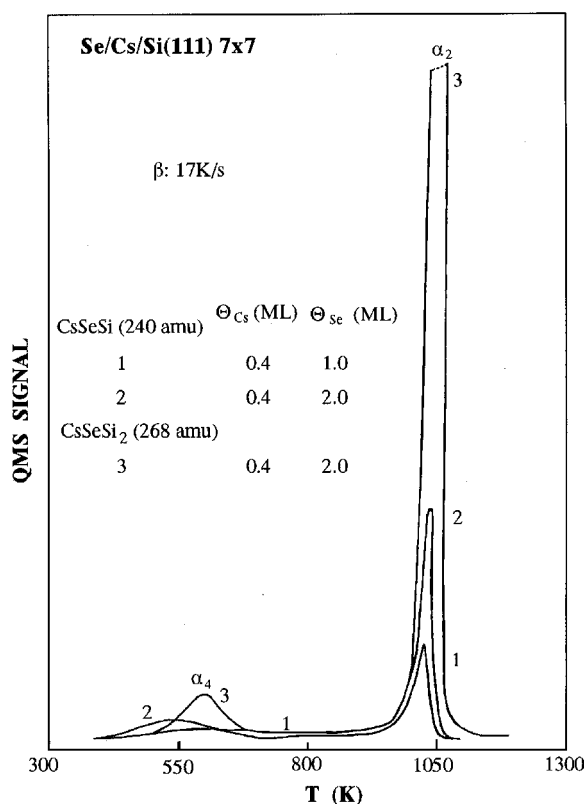


Figure 7. This figure shows a series of TDS of CsSeSi (240 amu) and CsSeSi₂ (268 amu), desorbed from Se/Cs/Si(111)-7 × 7 surfaces, at a constant heating rate, from 300 to 1300 K.

interest for that reason. Peak α_3 , on the other hand, exclusively involves the desorption of Se and SiSe (a result of SiSe fragmentation in the QMS), while peak α_4 is most probably due to Cs_xSe_ySi_z compounds at higher adsorbate coverage, forming a loosely bound overlayer on the substrate. The respective binding energies of all detected TDS peaks were calculated using Seebawer's formula [34]:

$$E_d = (k_B T_p)(0.5 + Y - \ln Y + \ln Y(2 - \ln Y)/2Y^2). \quad (1)$$

Here the desorption energy E_d is considered equal to the binding energy E_b ; $Y = \ln(vT_p/\beta)$, v is the pre-exponential factor, equal to 10^{13} s^{-1} , T_p the thermal desorption peak temperature, β the constant heating rate, equal to 17 K s^{-1} , and k_B Boltzmann's constant [35].

The first of the three peaks, which are common to the TDS of Cs and Se (as well as SiSe), is that which is labelled α_2 , observed at about 1050 K. This peak was detected in all our TDS observations and contains Cs, Se, SiSe, Cs, CsSe (not shown here) and Cs_xSe_ySi_z compounds (figures 4–7). As it is a common element in all our TDS measurements, it is safe to regard α_2 as the peak representing the desorption of Cs_xSe_ySi_z from the substrate surface at the observed temperature, possibly via an etching process, which removes large portions of the top surface layer intact. The other compounds detected at 1050 K are most probably due to the fragmentation of the larger desorbed portions of the Cs/Se/Si(111)-7 × 7 surface in the QMS. The calculated binding energy of peak α_2 is $E_{\alpha_2} = 2.8 \text{ eV/atom}$. This can be compared with the calculated binding energies of peak α_3 ($E_{\alpha_3} = 2.6 \text{ eV/atom}$), observed in the TDS of

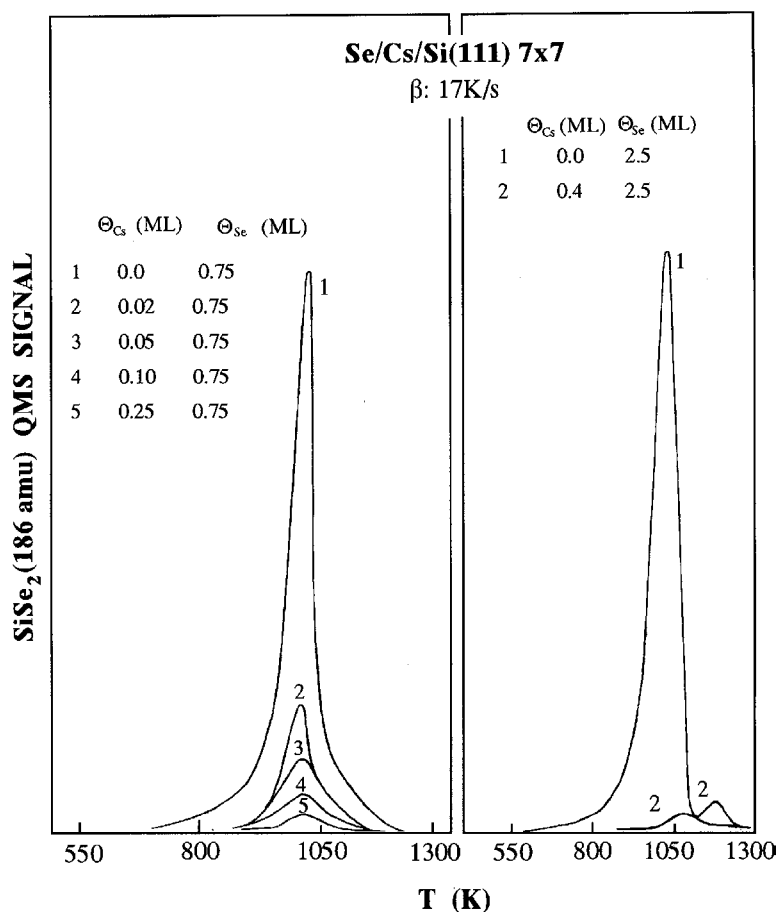


Figure 8. This figure depicts the TDS of $\text{SiSe}_2(186 \text{ amu})$ desorbed from $\text{Se/Si}(111)\text{-}7 \times 7$ and $\text{Se/Cs/Si}(111)\text{-}7 \times 7$ surfaces, at a constant heating rate, from 300 to 1300 K. On the left of the figure, Se coverage remains at a constant 0.75 ML. On the right side of the figure are the TDS of 2.5 ML of Se deposited onto clean and Cs-saturated $\text{Si}(111)\text{-}7 \times 7$ surfaces.

Se and SiSe (figures 5 and 6), and the peak of SiSe_2 desorbed from $\text{Se/Si}(111)\text{-}7 \times 7$ surfaces with a calculated binding energy of $E_{\text{SiSe}_2} = 2.7 \text{ eV/atom}$. The pertinent observation here is that the Se that would have gone into the formation of SiSe_2 on the Se-covered $\text{Si}(111)\text{-}7 \times 7$ surface instead interacts chemically with adsorbed Cs, while the rest of the Se remains on or near the surface, and forms a 1:1 stoichiometry with Si in the form of SiSe.

The next peak of interest desorbs at about 1100 K, and appears at the same coverage as α_2 . Peak α_1 is observed in the TDS of Cs, Se and SiSe (figures 4 and 6), but was not detected in the spectra of CsSe and CsSeSi compounds. Here we have apparently different substances desorbing at the same temperature, and hence having the same binding energy ($E_{\alpha_1} = 3.0 \text{ eV/atom}$). It is most likely, therefore, that the elements detected in the spectrometer are dissociated fragments of CsSeSi compounds. The absolute lack of presence of the latter compounds, moreover, suggests that most of the proposed dissociation either occurs immediately before or after desorption, i.e. *before* the removed material reaches the QMS. The mechanics of the aforementioned chemical dissociation may, therefore, be driven by the

activation energy provided by heating the surface to temperatures >1050 K. The cesium–selenium bonds, moreover, are the ones most likely to break in this case, leaving atomic Cs and SiSe to reach the QMS for detection. The detected Se is probably due to fragmentation of SiSe within the spectrometer.

From the comparison of the initial Cs (563 eV) Auger peak height at RT with that at 1100 K, we may surmise that upon the desorption of peak α_1 , Cs is at 30% of its RT saturation level (i.e. about 0.14 ML). In all likelihood, after the desorption of substances corresponding to peak α_2 at 1050 K, the remaining Cs reforms the compounds with Se and Si that were previously detected. The same process probably occurs after the materials of peak α_1 are removed. The interesting feature of peak α , however, lies in its comparison with a corresponding high-temperature peak of Se (and SiSe), which appears when Se is adsorbed on clean Si(111)- 7×7 and the resulting surface is subsequently heated to about 1190 K (with a calculated Se surface binding energy of about 2.9 eV/atom) [21]. This peak saturates at $\Theta_{\text{Se}} \cong 0.50$ ML, and represents the Se which preserves the heated Si(111)- 7×7 surface in its restored 1×1 bulk-terminated state, by adhering to the dangling bonds of the 1×1 surface [21]. For the Cs/Se/Si(111)- 7×7 heated surface, peak α appears at about 1210 K (with a binding energy calculated at about $E_\alpha = 3.2$ eV/atom). The presence of Cs alters this high-temperature Se peak by causing a small shift to higher binding energies (by about 0.3 eV/atom). The main influence, however, of the presence of Cs on the high-temperature Se (and SiSe) TDS peak is that it removes the latter peak's 0.50 ML saturation limit for Se. In other words, even at $\Theta_{\text{Cs}} \cong 0.14$ ML (after heating the Se/Cs/Si(111)- 7×7 surface to 1100 K) the presence of Cs causes the intensity of peak α to increase indefinitely with increasing Se coverage, while, as was previously mentioned, inhibiting the diffusion of Se below the top surface layer (verified by WF and LEED observations). The reason for this may be the tendency of Cs to retain Se on the top surface layer where its binding to the substrate is apparently stronger. Moreover, this increased presence of Se on the Cs/Si(111)- 7×7 surface after heating to 1100 K may contribute to the observed disorder also being restricted to the top surface layer.

Besides being detected in the temperature range of peak α_2 , CsSeSi and CsSeSi₂ are also detected between 450 and 600 K, with a maximum binding energy of 1.6 eV/atom (peak α_4), for varying adsorbate coverages (figure 7). Cesium does not occupy the top positions at these temperatures (WF measurements of figure 3, right), and these loosely bound CsSeSi complexes are most probably formed by CsSe bonding to stray Si atoms diffusing from the bulk. It is noteworthy, furthermore, that the small amounts of SiSe₂ detected at a RT Se coverage of 2.5 ML (when $\Theta_{\text{Cs}} \cong 0.47$ ML) were represented by two peaks with calculated binding energies of 2.9 and 3.1 eV/atom. These two very small peaks of SiSe₂ are possibly associated with the corresponding binding states of Cs, Se and SiSe represented by peaks α_1 and α .

In concluding, we find it pertinent to make one final observation regarding the positioning of peaks α , α_1 and α_2 along the thermal spectrum with respect to the behaviour of the heated Si(111)- 7×7 surface. It is well known that the clean Si(111)- 7×7 undergoes a $7 \times 7 \rightarrow 1 \times 1$ phase transition, observed at about 1130 K [20]. When Se at a $\Theta_{\text{Se}} \geq 0.50$ ML coverage is present on the latter surface, however, this transition temperature shifts to the 1050–1100 K range. It is unknown whether a similar structural transition occurs after the coadsorption of Cs and Se on Si(111)- 7×7 surfaces. There are, however, three observed binding states common to Cs and SiSe (and most probably their compounds), which correspondingly occur before (peak α_2), during (peak α_1) and after (peak α) the structural transition observed on heated Se/Si(111)- 7×7 surfaces. With this coincidence in mind, we may suggest that even with Cs and Se present as adsorbates on its surface, Si(111)- 7×7 may still retain the tendency toward surface modification, possibly exhibited as a surface relaxation, at temperatures >1050 K, and

that this modification may influence the desorption process in a catalytic manner resulting in the observed binding states represented by peaks α , α_1 and α_2 .

4. Conclusions

This investigation is a study of the room and elevated temperature structural and chemical interactions between Se, Cs and Si, when Se is adsorbed at RT on Cs/Si(111)-7 × 7 surfaces of varying Cs coverage. The investigation was conducted in UHV utilizing the surface analysis techniques of AES, LEED, WF measurements and TDS. Adsorption of Se on the Cs/Si(111)-7 × 7 surface at $\Theta_{\text{Cs}} \cong 0.47$ ML (Cs saturation) results in Se being initially adsorbed on the bare portions of the disordered Si(111)-7 × 7 surface (until $\Theta_{\text{Se}} \cong 0.50$ ML), and subsequently on the Cs adlayer, in the centre of the disordered 7 × 7 unit-cell domain. Selenium adatoms on caesiated surfaces do not diffuse into the substrate bulk when $\Theta_{\text{Se}} > 0.50$ ML, but remain on the top surface layer. This includes Se adatoms adsorbed on the bare portions of the Si(111)-7 × 7 surface. The adsorption of Se on Cs/Si(111)-7 × 7 surfaces at RT greatly increases the already present surface disorder.

Heating the Se/Cs(0.47 ML)/Si(111)-7 × 7 surface ($0.50 \text{ ML} \leq \Theta_{\text{Se}} \leq 2.0 \text{ ML}$), up to 600 K causes a structural rearrangement, where Se begins to diffuse between Cs adatoms and the Si surface atoms. At $\Theta_{\text{Se}} \cong 2.0$ ML, a proportion of Se adatoms bond with Cs and possibly with Si atoms that have diffused upward from the substrate bulk and are removed from the surface (with a calculated binding energy of about 1.6 eV/atom). At higher temperatures (up to 1000 K), Se resting on the bare portions of the Si(111)-7 × 7 substrate forms SiSe with the substrate (unless compound formation has already occurred at lower temperatures), and is subsequently removed from the surface. The activation energy provided by the increased temperatures causes Se to form strong dipoles with Cs, and most probably a strengthening of the Se bonding to the Si substrate atoms directly below it. The bonds are strong enough that the Cs–Se–Si chains remain intact when they are thereafter removed from the surface at 1050 K. This removal resulted in the detection of CsSe and $\text{Cs}_x\text{Se}_y\text{Si}_z$ compounds at the latter temperature.

The presence of Se increases the binding energy of Cs on Si(111)-7 × 7 surfaces, while the binding energy of Se remains approximately equal to that on the clean Si(111)-7 × 7 surface. This may indicate that the increase in binding energy is due to Cs–Se bond formation. The presence of Cs on the Si(111)-7 × 7 surface also greatly suppresses the formation of SiSe₂ observed during the heating of Se/Si(111)-7 × 7 surfaces when $\Theta_{\text{Se}} > 0.50$ ML. At temperatures higher than 1050 K, CsSe compounds are not detected. However, two more binding states are observed for Cs and Se. These correspond to substrate binding energies of 3.0 and 3.2 eV/atom, and most probably result in the breaking of the Cs–Se bonds of the previously detected compounds (removed at 1050 K) before removal from the surface. To the extent, moreover, that Cs is present, CsSe compounds probably reform as the substrate surface cools below 1050 K. The presence of Cs, furthermore, keeps most of the adsorbed Se bonded to the Si surface layer at a high binding energy (3.2 eV/atom), in contrast to the case for the correspondingly strongly bonded Se on Si(111)-7 × 7 surfaces, which saturates at 0.50 ML, while higher Se coverage results in interdiffusion.

References

- [1] Dev B N, Thundat T and Gibson W M 1985 *J. Vac. Sci. Technol. A* **3** 945
- [2] Bringans R D and Olmstead M A 1989 *J. Vac. Sci. Technol. B* **7** 1232
- [3] Bringans R D and Olmstead M A 1989 *Phys. Rev. B* **39** 12 985

- [4] Mohapatra S M, Dev B N, Mishra K C, Gibson W M and Das T P 1988 *Phys. Rev. B* **38** 13 335
- [5] Papageorgopoulos A C and Kamaratos M 2000 *Surf. Sci.* **466** 173
- [6] Papageorgopoulos A C and Kamaratos M 2002 *Surf. Sci. Lett.* at press
- [7] Meng Shuang, Schroeder B R and Olmstead M A 2000 *Phys. Rev. B* **61** 7215
- [8] Proix F, Panella V, El Monkad S, Glebor A, Lacharme J P, Eddriel M, Amimer K, Sebenne C A and Toennies J P 1998 *Eur. Phys. J. B* **5** 919
- [9] Tuttle R, Ward J S, Duda T, Berens T A, Contreras M A, Ranganathan K R, Tennant A L, Keane J, Emery K and Nouf R 1996 *MRS Proc.* vol 426 (Pittsburgh, PA: Materials Research Society) p 143
- [10] Desplat J L and Papageorgopoulos C A 1980 *Surf. Sci.* **92** 97
- [11] Papageorgopoulos C A 1982 *Phys. Rev. B* **25** 3740
Papageorgopoulos C A 1989 *Phys. Rev. B* **40** 1546
- [12] Hatsopoulos C N and Gyftopoulos E P 1979 *Thermionic Conversion* (Cambridge, MA: MIT Press)
- [13] Yamazaki H and Nakamuro S-I 1999 *Phys. Rev. B* **59** 12 298
- [14] Luth H 1995 *Surfaces and Interfaces of Solid Materials* 3rd edn (Berlin: Springer)
- [15] Gorelik D, Aloni A, Eitle J, Meyler D and Haase G 1998 *J. Chem. Phys.* **108**, **23** 9877
- [16] Faraci G, Pennisi A R and Margaritondo G 1996 *Phys. Rev. B* **53** 13 851
- [17] Papageorgopoulos C A, Kamaratos M and Papageorgopoulos A 1998 *Surf. Sci.* **402** 120
- [18] Papageorgopoulos C A, Kamaratos M and Papageorgopoulos A C 1999 *Surf. Sci.* **433** 806
- [19] Papageorgopoulos A, Mosby D and Papageorgopoulos C A 1998 *Surf. Rev. Lett.* **5** 85
- [20] Telieps W and Bauer E 1985 *Surf. Sci.* **162** 163
- [21] Lifshits V G, Saranin A A and Zotov A X 1994 *Surface Phases on Silicon: Preparation, Structures and Properties* (Chichester: Wiley)
- [22] Oura K, Lifshits V G, Saranin A A, Zotov A V and Katayama M 1999 *Surf. Sci. Rep.* **35** 1–69
- [23] Magnusson K O, Wiklund S, Dudde R and Reihl B 1991 *Phys. Rev. B* **44** 5657
- [24] Etelaniemi V, Michel E G and Materlik G 1991 *Phys. Rev. B* **44** 4036
- [25] Hansen P E, Podersen K, Lin L and Morgen P 1997 *Surf. Sci.* **991** 252
- [26] Stauffer L and Minot C 1995 *Surf. Sci.* **331** 606
- [27] Cho K and Kaxiras E 1998 *Surf. Sci.* **396** L261
- [28] Clotet A, Ricart J M, Robio J and Illas F 1995 *Phys. Rev. B* **51** 158
- [29] Rannrez R 1989 *Phys. Rev. B* **40** 3962
- [30] Han Senng-Jin, Park Chan Seong, Lee Jong-Gyu and Kang Heon 2000 *J. Chem. Phys.* **112** 8660
- [31] Johansson L S and Reihl B 1993 *Surf. Sci.* **287** 524
- [32] Lee K D, Ahn J R and Chung J W 1999 *Appl. Phys. A* **68** 115
- [33] Papageorgopoulos A C and Kamaratos M 2001 *Surf. Rev. Lett.* **8** 633
- [34] Seebawer E G 1994 *Surf. Sci.* **316** 331
- [35] Horkmans A, Overbasch E G and Has J 1976 *Surf. Sci.* **59** 488